

# Structural investigations of bulk undoped and Ni doped ZnO samples: Role of NiO Secondary phase

Muzzammil Ahmad Bhat<sup>1\*</sup>, Shabir Ahmad<sup>2</sup>, Mohd. Nasir<sup>3</sup>

<sup>1</sup>Department of Physics, RDVV, Jabalpur-482001, (India)

<sup>2,3</sup>Department of Physics, Jamia Millia Islamia, New Delhi-110025, (India)

## ABSTRACT

*In the present paper we have performed the structural analysis of the undoped and Ni doped ZnO bulk samples. The X-ray diffraction measurements reveal the formation of the polycrystalline wurtzite phase of ZnO. From the detailed investigation it is observed that incorporation of Ni in ZnO matrix leads to the increase in the lattice parameter  $c$  which is reflected as a shift in the XRD peak of NiZnO towards lower Bragg angle. EDAX results confirm the presence of Ni with effective atomic percentage of  $3.84 \pm 0.8\%$ . Incorporation of Ni leads to the structural distortion in the host matrix.*

**Keywords:** X-ray diffraction, Lattice parameter, Disorder, Braggs Law, EDAX

## 1.INTRODUCTION

Zinc oxide (ZnO) has established itself as the promising candidate material for making blue light laser sources [1, 2]. The versatility of the material lies in the fact that apart from having large band gap and large exciton binding energy, this material is also chemically stable and is environment friendly [3]. Band gap engineering in ZnO is possible by suitably doping with Cadmium (Cd) or Magnesium (Mg) [4-6]. Room temperature ferromagnetism is also reported in ZnO when doped with Co, Ni, and Mn [7, 8] and makes it an important candidate in the field of diluted magnetic semiconductors (DMSs) which have potential applicability in emerging spintronics devices [9]. It has been reported that doping ZnO with Ni not only gives room temperature ferromagnetism, but it also causes lowering of the band gap. Combining these two properties can lead to the formation of heterostructures which will give rise to spin specific potential barrier heights to the carriers. NiO is also an important semiconductor exhibiting a typical p-type conductivity, which is attributed to the plentiful intrinsic acceptor defects [10-14] and has band-gap of 3.7 eV. Some groups have also observed a spin-glass or a paramagnetic behavior in their Ni doped samples [15].

Apart from all the investigations and observations, the successful growth of single phase TM ion doped ZnO is still a challenging task. Various important properties and characteristics of ZnO derived systems like room temperature ferromagnetism, high conductivity, and optical transparency are believed to be mainly influenced by the TM ion doping and the modifications in intrinsic defect levels. Due to low solubility limit of TM ions in ZnO, it is somehow difficult to avoid the secondary phase formation. In this scenario it becomes imperative to investigate and characterize the TM ion oxide phases in ZnO matrix. In the present work, we report the

structural analysis of undoped and Ni doped ZnO (Ni= 3%) by performing X-ray diffraction measurement. Energy dispersive X-ray analysis has been carried out to confirm the contents of elements present in the grown samples.

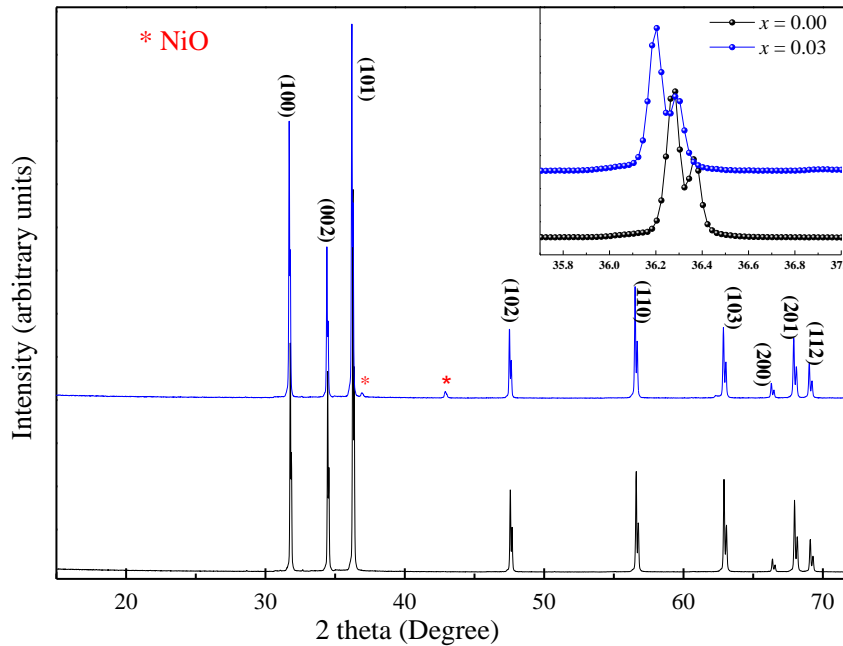


Figure 1: X-ray diffraction pattern of undoped and Ni doped ZnO bulk samples. Inset shows the zoomed view of peak corresponding to Bragg angle  $\approx 36^\circ$ . \* represents the peaks corresponding to NiO phase. The inset reveals a clear shift of the peak towards lower Bragg angle when doped with Ni.

## II. EXPERIMENTAL WORK

Pure ZnO and  $\text{Ni}_{0.03}\text{Zn}_{0.97}\text{O}$  bulk targets were prepared by standard solid-state reaction methods. For preparation the stoichiometric amounts of starting chemicals using commercial grade powders of ZnO (99.9%) and NiO (99.9%) as starting chemicals and were mixed thoroughly following by calcination at  $800^\circ\text{C}$  for 12 h following several cycles of dry grinding. The obtained powders were pressed into pellets of 5 g by weight and 25mm diameter at a pressure of  $5\text{tons}/\text{cm}^2$ . Prepared pellets were sintered at  $1400^\circ\text{C}$  for 24 h to remove the volatile and other low-temperature volatiles (if present). The samples were characterized for structural analysis by X-ray diffraction (XRD) using a Bruker X-ray diffractometer. For elemental analysis, energy dispersive x-ray analysis was performed. The targets were finally made in the form of 25 mm diameter pellets. prepared.

## III. RESULTS AND DISCUSSIONS;

Fig.1. Shows the typical XRD pattern of the as-synthesized ZnO and Ni doped ZnO bulk samples. Both the samples are polycrystalline in nature and the preferred structure correspond to wurtzite phase of ZnO. However apart from ZnO, two minor peaks corresponding to NiO are also observed. This is mainly attributed to the low solubility limit of 3d impurities in ZnO matrix [16]. In ZnO, Zn has the coordination number 4, having an

atomic radius of 0.74 Å [17] and forms a stable oxidation state of +2 [18]. However, due to smaller ionic radii of Ni<sup>2+</sup> (0.69 Å), becomes very much unstable in the ZnO matrix. Consequently, it has the tendency to form clusters of metallic Ni or NiO as is evident in the XRD pattern. It is also observed that the (002) peak of NiZnO sample is shifted towards lower diffraction angle as compared to pure ZnO. The FWHM of the Ni doped ZnO is also increased as compared to pure ZnO (0.063 for ZnO and 0.065 for NiZnO). This is mainly attributed to the formation of NiO secondary phase in ZnO matrix. Also, these changes are well reflected in the broadening of the peak which might occur due to the reduction in grain size and due to the disorderness present in the Ni doped ZnO [19] which are in well agreement with ours results. The shifting of the diffraction peak along with the variation of the lattice parameter also hints at the possibility of the incorporation of Ni at Zn site in ZnO matrix.

To explore the effects of Ni doping in ZnO on its crystal structure we have also calculated the lattice parameters from the XRD pattern. According to Bragg's law, [20] the lattice parameter of hexagonal bulk samples can be calculated by;

$$\sin^2 \theta = \frac{\lambda^2}{4} \left( \frac{4}{3} \frac{h^2 + hk + k^2}{a^2} + \frac{l^2}{c^2} \right) \quad 1$$

For the (002) orientation at  $2\theta \approx 34.4^\circ$ , the lattice constant "c" can be calculated by;

$$c = \frac{\lambda}{\sin \theta} \quad 2$$

using equation (2) the lattice parameter of ZnO and Ni doped ZnO samples are found to be 5.19 Å and 5.20 Å, respectively. Our observations reveal a shift in the lattice parameter indicating that the lattice parameter of the NiZnO sample increases slightly as compared to pure ZnO. It can be concluded that despite of the smaller ionic radii of the Ni<sup>2+</sup> as compared to Zn<sup>2+</sup> there is a slight increase in the lattice parameter c. This can be understood in terms of the distortion/disorder in the unit cell due to the formation of the NiO secondary phase. Also, the high electronegativity of NiO contributes to the distortion in the system.

We have also calculated the average grain size (D) by using the Debye Scherrer's formula as given below;

$$D = \frac{k\lambda}{\beta \cos(\theta)} \quad 3$$

Where k is a constant equal to 0.91 for temperature independent measurements. λ is the wavelength of the incident radiation which is 1.54106 Å for Cu Kα in the present case. β is the full width at half maxima in radians and θ is the Bragg angle. From our calculations it is observed that the grain size decreases when ZnO is doped with Ni. These results are in corroboration with the earlier reported trend [21]. The grain size is reduced in Ni doped sample as compared to the pure ZnO. The results reveal that Ni doped ZnO samples can reduce the average crystallite size because of the decrease in the reactant mobility with increased Ni content arising due to larger Ni-O bonding compared to Zn-O bonding energy [22].

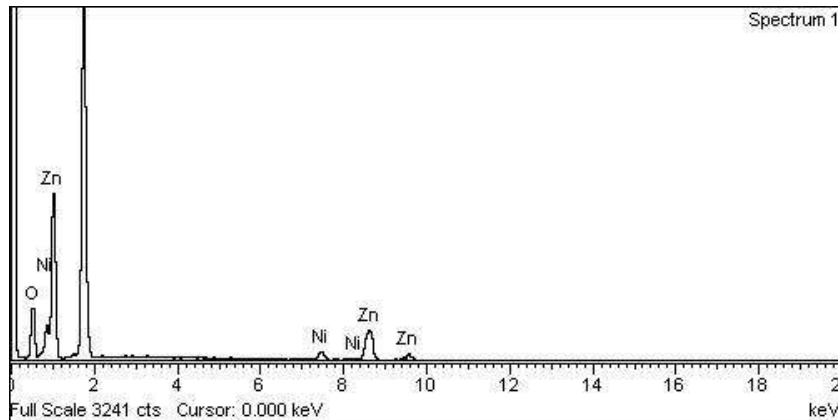


Figure 2. EDAX spectra of Ni doped ZnO sample.

In order to further verify the existence of Ni in Ni doped sample, we have performed Energy dispersive x-ray (EDAX) analysis. Fig. 2 shows the EDAX of the NiZnO sample. It is evident that apart from other elements like Zn, Oxygen, Ni is also present in the sample and is  $3.84 \pm 0.8$  atomic %. The complete composition and the corresponding concentration is shown in Table 1.

Element	App	Intensity	Weight%	Weight%	Atomic%
	Conc.	Corrn.		Sigma	
O K	46.14	1.0838	36.96	1.12	70.28
Ni K	9.90	1.1604	7.41	0.71	3.84
Zn K	56.88	0.8878	55.63	1.31	25.89
Totals			100.00		

Table 1: Elemental composition in NiZnO sample as obtained from EDAX spectra

#### IV.CONCLUSION

The detailed structural analysis and the role of minor NiO secondary phase in ZnO matrix has been performed by performing XRD measurements. EDAX analysis shows that Ni is present with an effective concentration of  $3.84 \pm 0.8$  atomic%. It is observed that the incorporation of Ni in ZnO matrix leads to the strain and disorderness resulting in the large grain size and increased lattice parameter. The c parameter of samples is in close agreement to the reported literature.

## REFERENCES

- [1.] Y. Segawa, A. Ohtomo, M. Kawasaki, H. Koinuma, Z.K. Tang, P. Yu, G.K.L. Wong, *Phys. Stat. Sol. B* 202 1997, 669.
- [2.] G. Du, Y. Cui, X. Xiaochuan, X. Li, H. Zhu, B. Zhang, Y. Zhang, Y. Ma, *Appl. Phys.Lett.* 90 (2007) 243504
- [3.] AJanotti, Chris G. Van de Walle, *Rep. Prog. Phys.* 72, 2009, 126501
- [4.] T.H. Kim, J.J. Park, S.H. Nam, H.S. Park, N.R. Cheong, J.K. Song, S.M. Park, *Appl. Surf. Sci.* 255, 2009, 5264
- [5.] N.S. Minimala, A. John Peter, *J. Nano- Electron. Phys.* 4, No 4, 2012, 04004
- [6.] J.R. Ray, M.S. Desai, C.J. Panchal, P.B. Patel, *J. Nano- Electron. Phys.* 3, No 1, 755 (2012)
- [7.] H. Ohno, *Science* 281, 1998, 951
- [8.] Y. Matsumoto, M. Murakami, T. Shono, T. Hasegawa, T. Fukumura, M. Kawasaki, P. Ahmet, T. Chikyow, S.Koshihara, and H. Koinuma, *Science* 291, 2001, 854.
- [9.] J.K. Furdyna, Diluted magnetic semiconductor thin films and multilayers, *MRS Proc.*517, 1998, 613
- [10.] H. Sato, T. Minami, S. Takata and T. Yamada, *Thin Solid Films* 236, 1993, 27
- [11.] H. Ohta, M. Hirano, K. Nakahara, H. Maruta, T. Tanabe, M. Kamiya, T. Kamiya and H. Hosono, *Appl. Phys. Lett.* 83, 2003, 1029
- [12.] Z. J. Zhang, Y. Zhao and M. M. Zhu, *Appl. Phys. Lett.* 88, 2006, 033101
- [13.] Y. H. Park, Y. H. Shin, S. J. Noh, Y. Kim, S. S. Lee, C. G. Kim, K. S. An and C. Y. Park, *Appl. Phys. Lett.* 91, 2007, 012102
- [14.] K. Wang, Y. Vygranenko and A. Nathan, *Thin Solid Films* 516, 2008, 1640
- [15.] C. G. Van de Walle, *Phys. Rev. Lett.* 85, 2000, 1012
- [16.] T.Wakano, N.Fujimura, Y.Morinaga, N.Abe, A.Ashida, T.Ito, *Physica E*, 10,2001, 260
- [17.] J. Mohapatra, D. K. Mishra, S. K. Kamilla, V. R. R. Medicherla, D. M. Phase, V. Berma, and S. K. Singh, *Phys. Status Solidi B* 248, 6, 2011, 1352–1359.
- [18.] R. D. Shanon, *Acta Crystallogr. A* 32, 1976, 751–756.
- [19.] A. Agrawal, T. A. Dar, P. Sen, and D. M. Phase, *J. Appl. Phys.* 115, 2014, 143701.
- [20.] F. K. Shan, B. I. Kim, G. X. Liu, Z. F. Liu, J. Y. Sohn, W. J. Lee, B. C. Shin and Y. S. Yu, *J. Appl. Phys.* 95, 2004, 4772.
- [21.] T. A. Dar, A. Agrawal, P. Misra, L. M. Kukreja, P. K. Sen, P. Sen, *Current Applied Physics* 14, 2014, 171-175.
- [22.] J. A. Peters, N.D. Parashar, N. Rangaraju, B.W. Wessels, *Phys. Rev. B* 82, 2010, 205207.